Preparation, Characterization, and Self-Assembled Properties of Biodegradable Chitosan−Poly(L-lactide) Hybrid Amphiphiles

Hao Feng and Chang-Ming Dong*

Department of Polymer Science & Engineering, School of Chemistry and Chemical Technology, Shanghai Jiao Tong University, Shanghai 200240, People's Republic of China

Received June 14, 2006; Revised Manuscript Received August 23, 2006

Biodegradable chitosan-*graft*-poly(L-lactide) (CS-*g*-PLLA) hybrid amphiphiles were prepared through direct grafting of a PLLA precursor to the backbone of CS. The average number of PLLA grafts per CS could be adjusted by the feed ratio of PLLA to CS, and it varied from 1.3 to 16.8. Moreover, both the crystallization rate and degree of crystallization of PLLA grafts with these graft copolymers could be adjusted by the chain length of PLLA and the number of PLLA grafts per CS, respectively. Meanwhile, CS-*g*-PLLA exhibited good solubility in some nonpolar and polar organic solvents compared with the original CS. Furthermore, self-assembled nanoparticles could be generated by direct injection of these graft copolymer solutions into distilled water, and their critical aggregation concentration decreased with increasing number of PLLA grafts per CS. The average size of the nanoparticles (25−103 nm) could be adjusted through the graft copolymer composition and the graft copolymer concentration, which was very different from the observations in ordinary PLLA-*b*-poly(ethylene oxide) amphiphiles. Significantly, this will provide a convenient method not only to combine the bioactive functions of CS with the good mechanical properties of biodegradable polymers, but also to generate nanoparticles with adjustable sizes for targeted drug release.

Introduction

Supramolecular self-assembly of amphiphilic block copolymers can generate a variety of hierarchical nanoscale aggregates, which hold great potential in drug delivery vesicles, diagnostic biosensors, and tissue engineering.[1−4] For these purposes, designing diverse amphiphilic biocompatible and biodegradable polymeric amphiphiles has been increasingly exploited worldwide. For example, synthetic biodegradable polylactide/poly(ethylene oxide) (PEO) and poly(ϵ-caprolactone)/PEO amphiphiles have been investigated in detail to generate diverse nanoaggregates including spherical micelles, cylinders, and polymersomes (bilayered vesicles).[5] However, studies on biohybrid amphiphiles composed of natural water-soluble biomacromolecules and hydrophobic biodegradable polymers (such as FDA-approved polylactides and poly(ϵ-caprolactone)) are still limited. Chitosan (CS) is the fully or partially deacetylated polysaccharide of a naturally abundant chitin, known to be biocompatible, biodegradable, and bioactive in animal/human tissues. Recently, much attention has been paid to utilizing CS and its derivatives for drug delivery vehicles, wound healing accelerators, and nerve regeneration agents.[6−8] Despite these advantageous potentials of CS, both its poor mechanical and processing properties and its insolubility in common organic solvents have delayed its basic research and various biofabrication applications. Therefore, it is urgent to generate CS-based biohybrid amphiphiles.[9−11]

Owing to its good mechanical properties, biodegradable poly(L-lactide) (PLLA) has been widely used in surgical sutures, drug delivery systems, and tissue engineering.[12,13] However, the high crystallinity, the strong hydrophobicity, and especially the lack of bioactive functions of the PLLA matrix often resulted in an uncontrollable biodegradation rate and an undesirable biological response to cells and/or tissues. Therefore, it is promising to combine the bioactive functions of CS with the good mechanical properties of PLLA to generate a new kind of biohybrid amphiphile. Meanwhile, the hydrophobicity−hydrophilicity balance of the CS−PLLA biohybrid can be easily adjusted by the graft copolymer composition, and it is expected to be fabricated into biodegradable nanoparticles.

Recently, CS-*g*-oligo(lactic acid) with a low grafting content was prepared via direct polycondensation of CS with L-lactic acid and ring-opening graft copolymerization of L-lactide with CS. For example, Albertsson et al. prepared pH-sensitive hydrogels based on CS-*g*-oligo(D,L-lactic acid) and/or CS-*g*-oligo(glycolic acid) using a polycondensation method, and the degree of substitution of the graft copolymer was low (<20%).[14,15] Yao et al. synthesized CS-*g*-oligo(L-lactic acid) through aldehyde-terminated oligo(L-lactic acid) with CS.[16] However, because of the short length of oligo(L-lactic acid), the mechanical and processing properties of the synthetic polymer cannot be endowed to the backbone of CS. In this paper, CS-*g*-PLLA biohybrids with a long chain length of PLLA were prepared via a direct "graft-to" strategy (Scheme 1), and they were characterized in detail. The average size of the self-assembled nanoparticles (generally less than 100 nm) can be adjusted by the number of PLLA grafts per CS (i.e., the graft copolymer composition) and the graft copolymer concentration in solution. This is very different from amphiphilic PLLA-*b*-PEO and/or poly(ϵ-caprolactone)-*b*-PEO systems, where different copolymer compositions would mainly induce the morphological evolution of self-assembled aggregates (e.g., the morphology typically changed from spherical micelles to cylinders to vesicles).[5] Significantly, this will provide a convenient method not only to combine the bioactive functions of CS with the good mechanical properties of biodegradable polymers, but also to generate nanoparticles with adjustable sizes for targeted drug release.[17]

* To whom correspondence should be addressed. Phone: 86-21-54748916. Fax: 86-21-54741297. E-mail: cmdong@sjtu.edu.cn.

10.1021/bm060568l CCC: $33.50
Published on Web 10/10/2006

Scheme 1. Synthesis of CS-*g*-PLLA Hybrid Amphiphiles via a Graft-To Strategy

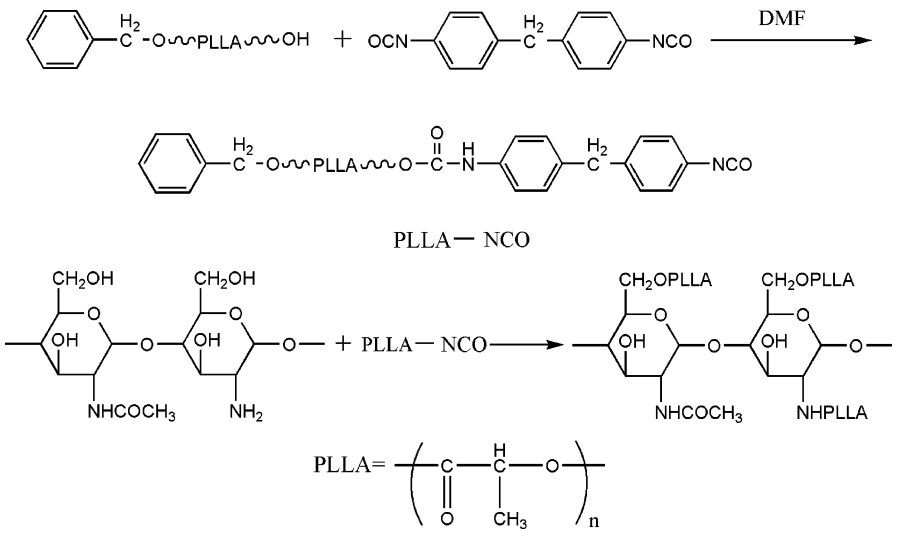

Experimental Section

Materials. CS (M_n = 5000, degree of deacetylation 80%) was purchased from Yuhuan Ocean Biochemal Ltd. (Zhejiang, China) and dried in a vacuum at 100 °C for 8 h prior to use. Well-defined PLLA terminated with hydroxyl groups ($M_{n,NMR}$ = 10000, polydispersity index 1.1) was synthesized from ring-opening polymerization of L-lactide (L-LA) using benzyl alcohol as an initiator and stannous octoate as a catalyst in bulk at 130 °C in the lab according to our previous paper.[18] 4,4′-Diphenylmethane diisocyanate (MDI; Aldrich) and tin(II) dibutyl dilaurate (Shanghai Kewang Chemicals Ltd., China) were used without further purification. Dimethylformamide (DMF) was distilled from calcium hydride under reduced pressure and stored over molecular sieves. 1,6-Diphenyl-1,3,5-hexatriene (DPH) was purchased from Aldrich and used as a probe molecule.

Methods. The FT-IR spectrum was recorded on a Fourier transform infrared spectrometer. ^{1}H NMR and ^{13}C NMR spectroscopy was performed on a Varian Mercury-400 spectrometer. Both CS and CS-*g*-PLLA graft copolymers were dissolved in d_6-DMSO solvent. The molecular weight distribution of CS-*g*-PLLA was determined on a gel permeation chromatograph (Perkin-Elmer Series 200) and a refractive index detector at 30 °C, with DMF as the eluent (1.0 mL/min) and polystyrene as the calibration standard. The differential scanning calorimetry (DSC) analysis was carried out using a Seiko DSC 6200 instrument. All samples were heated from 25 to 200 °C at 10 °C/min. Wide-angle X-ray diffraction (WAXD) patterns of powder samples were obtained at room temperature on a Shimadzu XRD-6000 X-ray diffractometer with a Cu Kα radiation source (wavelength 1.54 Å). The supplied voltage and current were set to 40 kV and 30 mA, respectively. Samples were exposed at a scan rate of $2\theta = 4$ deg min^{-1} between $2\theta = 5°$ and 40°. The crystallization morphology of the polymer was observed using a Leica DMLP polarized optical microscope (Leica Microsystems GmbH, Germany). The solution of sample in CH_2Cl_2 (4 mg/mL) was sandwiched between two glass plates after the solvent completely evaporated, heated to 170 °C, held for 3 min to erase the thermal history, and then quenched to the desired isothermal crystallization temperature at 130 °C. UV−vis absorption spectra of the samples were recorded at room temperature using a Spectrumlab54 UV−vis spectrophotometer. The mean size of the nanoparticles was determined by dynamic light scattering (DLS) using a Malvern Nano_S instrument (Malvern, U.K.). The solution of nanoparticles was performed at a scattering angle of 90° and at 25 °C. All the measurements were repeated three times, and the average values reported were the mean diameter ± standard deviation. Transmission electron microscopy (TEM) was performed using a JEM-2010/INCA OXFORD transmission electron microscope (JEOL/OXFORD) at a 200 kV accelerating voltage. Samples were deposited onto the surface of 200 mesh Formvar carbon film coated copper grids. Excess solution was quickly wicked away with a filter paper. The image contrast was enhanced by negative staining with phosphotungstic acid.

Preparation of an NCO-Terminated PLLA Precursor (PLLA−NCO). Both PLLA (158 mg) and MDI (5 mg, 1.4 equiv to PLLA) were put into a dried flask quickly. The flask was then connected to a Schlenk line, where an exhausting−refilling process was repeated three times. DMF (1 mL) was added to the mixture under a N_2 atmosphere, and then the reaction was kept at 60 °C with vigorous stirring for 2 h. The resulting telechelic PLLA−NCO solution was used immediately for the following grafting reaction.

Preparation of CS-*g*-PLLA. CS (10 mg) and DMF (0.5 mL) were put into a dried flask quickly. The flask was then connected to a Schlenk line, where an exhausting−refilling process was repeated three times. Then the above PLLA−NCO solution and tin(II) dibutyl dilaurate (0.2 mol % PLLA−NCO) were quickly transferred to the mixture under a N_2 atmosphere. The reaction was continued at 80 °C with vigorous stirring for 4 h and then cooled to room temperature. CS and CS-*g*-PLLA were insoluble in DMF and toluene at room temperature, respectively, so both the possibly unreacted CS and the possibly cross-linked CS were removed by simple filtration, and then PLLA−NCO or PLLA and tin(II) dibutyl dilaurate were extracted completely by a large amount of toluene for 4 h. The purified CS-*g*-PLLA was then dried in a vacuum at 100 °C for 8 h (101.0 mg, grafting yield of PLLA 57.5%).

Fabrication of Nanoparticles. A direct solution injection method was used to fabricate nanoparticles from CS-*g*-PLLA. Briefly, 1 mL of the CS-*g*-PLLA copolymer solution (5 mg/mL) in THF (except sample CS-*g*-PLLA1 in dioxane) was added dropwise to 10 mL of distilled water under vigorous stirring. THF was completely evaporated under reduced pressure, and then the nanoparticle solution was filtered through a 0.45 μm microfilter membrane to remove possible aggregates. The yield of nanoparticles was about 60%, and the mean size of the nanoparticles was determined by DLS at 25 °C.

Measurement of the Copolymer Critical Aggregation Concentration. The critical aggregation concentration (cac) of CS-*g*-PLLA amphiphiles was determined employing the hydrophobic dye solubilization method using DPH as a probe molecule.[19] DPH was dissolved in methanol to produce a 0.5 mM DPH/methanol solution. To a quartz cell were added 0.5 mL of copolymer nanoparticle solution and 5 μL of DPH solution, the cell was capped with a Teflon film, and the solutions were then allowed to homogenize for about 2 min at room temperature. To prevent the evaporation of water during the measurement, the sample cell was sealed with a Teflon film. UV−vis spectra of the samples were recorded in the 200−500 nm range at room temperature.

Table 1. Synthesis and Melting Properties of CS-*g*-PLLA Hybrid Amphiphiles

sample	CS/PLLA (feed ratio, g/g)	yield[a] (%)	T_m[b] (°C)	ΔH_m[c] (J/g)	X_c[d] (%)	PLLA/CS[e] (gravimetry)	PLLA/CS[f] (^{1}H NMR)
CS-*g*-PLLA1	1/3.75	35.4	149.5	46.1	49.3	1.3	1.8
CS-*g*-PLLA2	1/15	57.5	153.9,162.3	59.6	63.7	4.8	
CS-*g*-PLLA3	1/30	80.9	154.3,162.0	61.6	65.8	12.4	13.8
CS-*g*-PLLA4	1/60	54.7	154.5,162.6	62.9	67.2	16.8	
PLLA	0/1		159.2	73.3	78.3		

[a] The grafting yield of PLLA = $(W_{CS\text{-}g\text{-}PLLA} - W_{CS})/W_{PLLA}$. [b] T_m denotes the melting temperature of the graft copolymer in the DSC curve. [c] ΔH_m denotes the fusion enthalpy of the graft copolymer in the DSC curve. [d] X_c denotes the degree of crystallinity of the graft copolymer. $X_c = \Delta H_m/\Delta H_m^\circ$, with $\Delta H_m^\circ = 93.6$ J/g. [e] PLLA/CS denotes the number of PLLA grafts per CS molecule determined gravimetrically. [f] PLLA/CS was determined by ^{1}H NMR.

Results and Discussion

Preparation of CS-*g*-PLLA Hybrid Amphiphiles. It is known in the literature that natural biomacromolecule/synthetic polymer hybrids can be prepared via both "graft-from" and "graft-to" strategies.[20] However, the chain length of the polymer grafts usually is short (i.e., oligomer), and the mechanical and processing properties of synthetic polymers cannot be endowed to the backbone of natural biomacromolecules. Therefore, CS-*g*-PLLA amphiphiles with a long chain length of PLLA grafts were prepared through direct grafting of PLLA to the backbone of CS via a graft-to strategy, as shown in Scheme 1. Well-defined PLLA terminated with hydroxyl groups was converted into telechelic PLLA−NCO, and then it was grafted to the backbone of CS. ^{1}H NMR spectroscopy of PLLA−NCO was performed in $CDCl_3$ (see Supporting Information Figure S1). Comparing one benzyloxy end group (1, $PhCH_2O$) of PLLA−NCO with the other end group (5, MDI residue), the integral ratio of proton 1 to proton 5 was 1.03, which was very close to its theoretical value ($S_1/S_5 = 1.0$). This indicated that one NCO-terminated PLLA was successfully obtained, and the dimerization of PLLA could be negligible within the determination limit of ^{1}H NMR. This was reasonable because excess MDI was used for the preparation of the PLLA−NCO precursor in our experiments. The grafting reaction was performed under heterogeneous conditions because CS was partially swelled in DMF at 80 °C. The grafting yield of PLLA increased with increasing feed ratio of PLLA to CS, and then it decreased with more PLLA added (Table 1). This could be attributed to the following reasons. With increasing PLLA grafting to the backbone of CS, the resulting graft copolymers became progressively soluble in the solution. Meanwhile, the steric effect among the PLLA grafts would hinder the continuous PLLA grafting to CS when the number of PLLA grafts per CS was higher. Note that PLLA−NCO was necessarily contaminated by residual MDI, which might induce partial cross-linking of CS. The purification procedure of the resulting graft copolymers can be summarized as follows: both the possibly unreacted CS and the possibly cross-linked CS could be removed by simple filtration, and then PLLA−NCO or PLLA and tin(II) dibutyl dilaurate were extracted completely by a large amount of toluene.

Compared to the FT-IR spectrum of CS (Figure 1), that of the obtained CS-*g*-PLLA presented new absorption peaks around 1192, 1304, 1757, and 2977 cm^{-1}, which were assigned to the symmetric C−O−C stretching modes, the carbonyl group, and CH ($-CH(CH_3)$) of the PLLA grafts, respectively. This suggested that PLLA was grafted to the backbone of chitosan. Meanwhile, the relative intensity of hydroxyl and amino groups within chitosan at 3410 cm^{-1} grew less with increasing grafting content of PLLA, while that of carbonyl groups at 1757 cm^{-1} increased.

In comparison with that of CS, the ^{1}H NMR spectrum of the resulting chitosan-*g*-PLLA graft copolymer showed new proton signals at 5.20 and 1.45 ppm assigned to CH ($-CH(CH_3)$) and $-CH_3$ of the PLLA grafts, respectively (Figure 2). Meanwhile, both the new peak at 2.88 ppm (2″) and the new multiple peaks at 4.19 ppm (3′) showed that both amino and hydroxyl groups of chitosan indeed participated in the grafting reaction with the PLLA−NCO precursor. Note that the integral ratio of proton 2″ (CS backbone) to proton 9 (the end group of PLLA) was equal to 1/2.1, which was close to its theoretical value ($S_{2''}/S_9 = 1/2$). This indicates that no remaining PLLA was present in the CS-*g*-PLLA copolymer within the determination limit of ^{1}H NMR. This further confirmed that the final purified product was the graft copolymer and not the CS/PLLA blend. In addition, the ^{13}C NMR spectrum of the CS-*g*-PLLA copolymer showed the presence of both CS and PLLA components within the copolymer, and it was difficult to differentiate the purity of the copolymer by this technique (see Supporting Information Figure S2). Moreover, the gel permeation chromatography (GPC) measurement showed that there was a single elution peak with reasonable polydispersity ($M_w/M_n = 1.29$) for the CS-*g*-PLLA copolymer, which verified that the as-synthesized CS-*g*-PLLA was pure (see Supporting Information Figure S3). Furthermore, the grafting content of PLLA (the average number of PLLA grafts per CS molecule) within the copolymer could be determined by the relative proton intensity of the PLLA units and CS units, which was nearly in agreement with that determined gravimetrically (Table 1). On the basis of the ^{1}H NMR analysis, the average number of PLLA grafts per CS could be calculated as follows:

$$\text{PLLA grafts per CS} = \frac{29(S_7 + S_{7'})}{(2 \times 70)(S_2 + S_{2'} + S_{2''})}$$

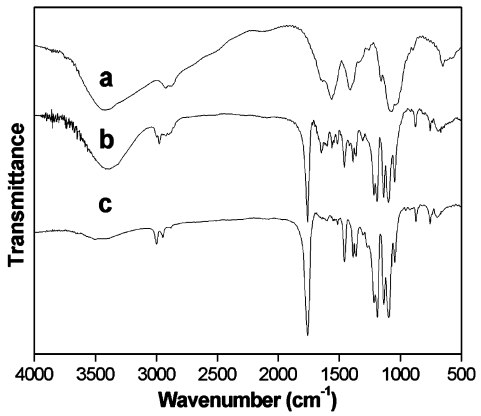

Figure 1. FI-IR spectra of CS and CS-*g*-PLLA copolymers: a, CS; b, CS-*g*-PLLA1; c, CS-*g*-PLLA2.

DSC and WAXD Analyses of CS-*g*-PLLA. The melting behaviors of these graft copolymers were investigated by DSC, as shown in Figure 3. The first heating scan in the DSC analysis

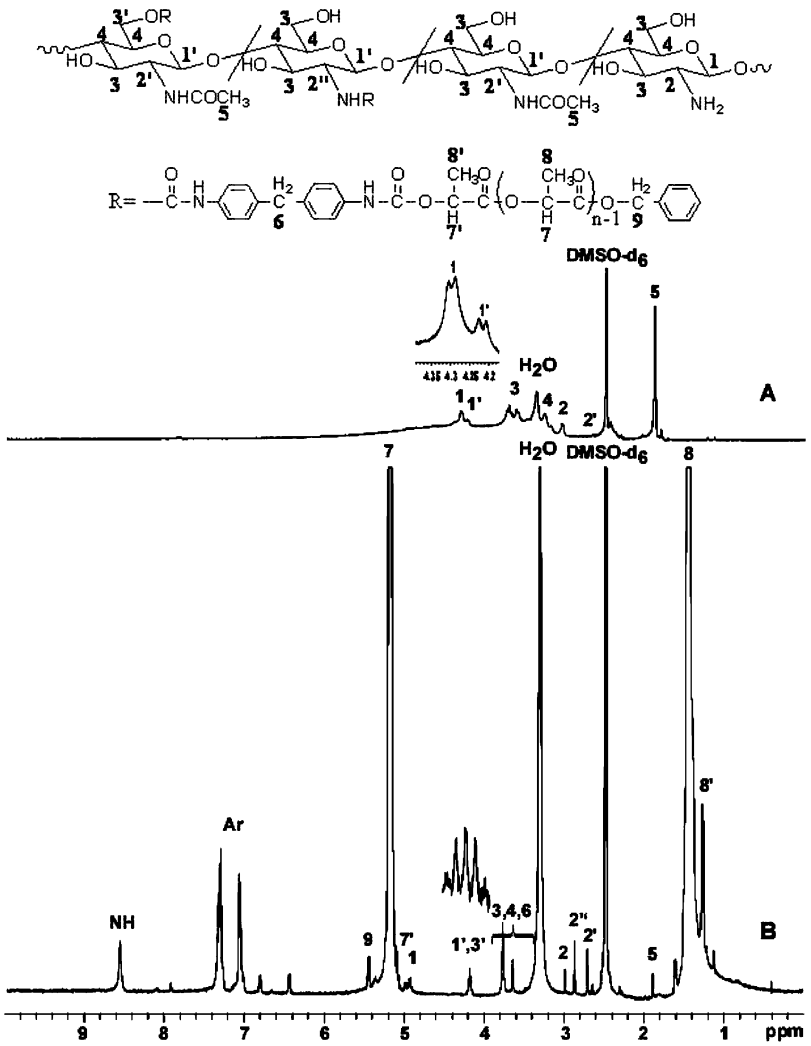

Figure 2. ^{1}H NMR spectra of CS (A) and CS-*g*-PLLA1 (B).

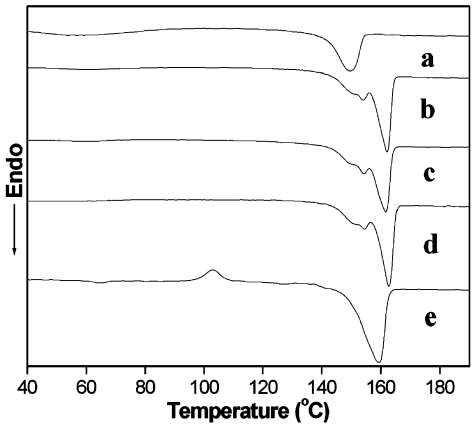

Figure 3. DSC curves of PLLA and CS-*g*-PLLA copolymers: a, CS-*g*-PLLA1; b, CS-*g*-PLLA2; c, CS-*g*-PLLA3; d, CS-*g*-PLLA4; e, PLLA.

was from 25 to 200 °C at a rate of 10 °C/min. CS-*g*-PLLA1 with a lower number of PLLA grafts presented a single lower melting point peak similar to that of the PLLA precursor, while there existed similarly two melting points in the DSC curves of samples CS-*g*-PLLA2, CS-*g*-PLLA3, and CS-*g*-PLLA4 with a greater number of PLLA grafts. This indicates that both the imperfect crystallization and/or the secondary crystallization existed in all samples excluding sample 1, which continued to rearrange and crystallize in the heating run.[18] The degree of crystallinity (X_c) of PLLA within these graft copolymers was determined from DSC analysis with the aid of the enthalpy of fusion of 93.6 J/g for the perfectly crystalline PLLA (Table 1). It can be concluded that X_c increased with increasing grafting content of PLLA, but it was less than that of the PLLA precursor. These results suggest that CS to some extent restricted the high crystallization of PLLA grafts within these copolymers.

WAXD is another useful method to demonstrate the structure of these graft copolymers in the solid state. CS showed two broad and weak diffraction peaks at $2\theta = 12°$ and 21°, while the graft copolymers apparently presented four new peaks at $2\theta = 14.5°$, 16.5°, 19°, and 21°, which were approximately the diffraction peaks of PLLA crystals (Figure 4).[21] This result is consistent with the DSC analysis, and these CS-*g*-PLLA graft copolymers formed micophase-separated crystalline materials (i.e., crystalline PLLA within graft copolymers) at room temperature. To clarify the crystallization behavior of PLLA grafts within CS-*g*-PLLA, the isothermal crystallization process was further investigated by the polarized optical microscopy (POM) technique.

POM Analysis. A polarized optical microscope was used to observe the crystalline morphology and the spherulitic growth process of CS-*g*-PLLA. The isothermal crystallization temperature was chosen at 130 °C, which was between T_m and T_c of the PLLA grafts. As shown in Figure 5, all the graft copolymers showed a spherulitic morphology with Maltese-cross patterns, which was similar to that of the pure PLLA precursor.[18]

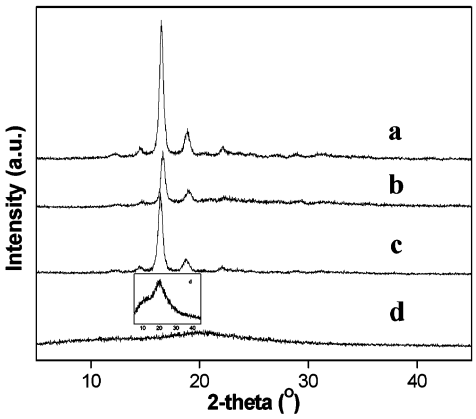

Figure 4. WAXD patterns of PLLA, CS, and CS-*g*-PLLA copolymers: a, CS-*g*-PLLA2; b, CS-*g*-PLLA1; c, PLLA; d, CS.

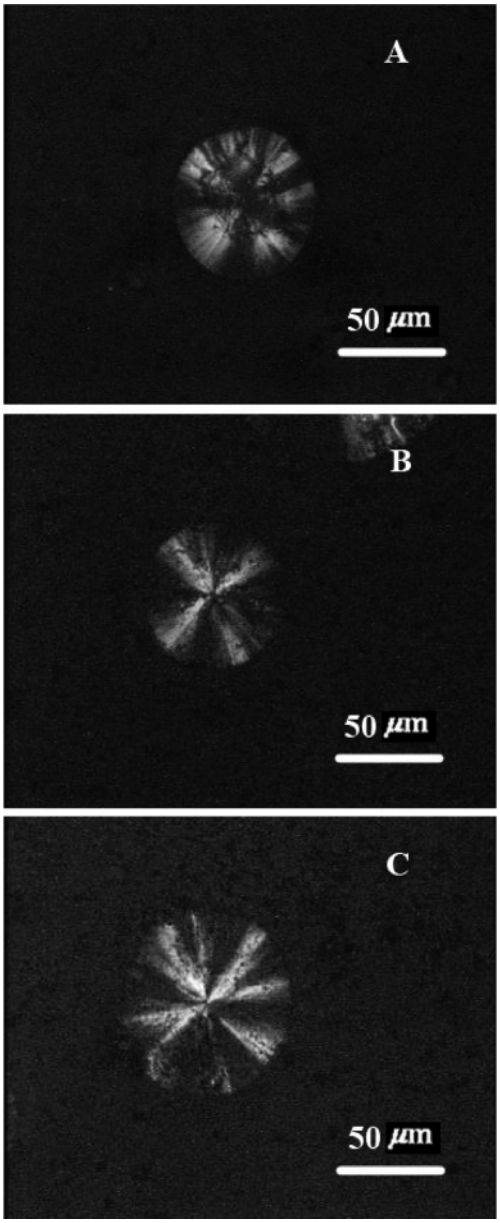

Figure 5. Spherulitic morphology of CS-*g*-PLLA copolymers isothermally crystallized at 130 °C: A, CS-*g*-PLLA2; B, CS-*g*-PLLA3; C, CS-*g*-PLLA4.

Moreover, the average radius of the spherulites was plotted against the isothermal crystallization time, as shown in Figure 6. The spherulitic radius linearly increased with the isothermal crystallization time, and the spherulitic growth rate (G) was evaluated from the slope of these lines. It is demonstrated that the spherulitic growth rate remained nearly constant (G = 0.33−0.41 μm/s), which indicated that the crystallization rate of the PLLA grafts within these copolymers mainly was controlled by the chain length of the PLLA grafts.[18,21,22] On the basis of the analyses of DSC, WAXD, and POM, it can be concluded that both the crystallization rate and degree of crystallization of these CS-*g*-PLLA copolymers could be adjusted by the chain length of PLLA and the number of PLLA grafts per CS, respectively. These are important parameters for adjusting the biodegradation rate and mechanical properties of biodegradable polymeric biomaterials.[23]

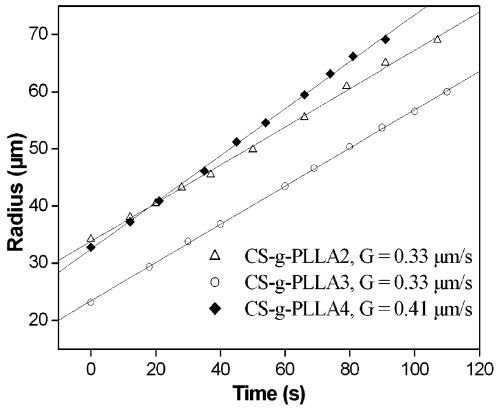

Figure 6. Dependence of the spherulite radius on the isothermal crystallization time for the CS-*g*-PLLA copolymers at 130 °C.

Table 2. Solubility of CS-*g*-PLLA in Common Polar and Nonpolar Organic Solvents[a]

sample	acetone	CH_2Cl_2	$CHCl_3$	THF	dioxane	DMF
CS-*g*-PLLA1	−	−	−	−	+	+
CS-*g*-PLLA2	−	+	+	+	+	+
CS-*g*-PLLA3	−	+	+	+	+	+
CS-*g*-PLLA4	−	+	+	+	+	+
CS	−	−	−	−	−	−

[a] The solubility tests were performed at room temperature, and the concentration was 5 mg/mL. Key: +, soluble; −, insoluble.

In all, the above results indicate that CS-*g*-PLLA hybrid amphiphiles were successfully synthesized via a convenient graft-to strategy, and PLLA grafts existed in a crystalline state within these copolymers. This investigation was different from those in previous papers,[9,16] where amorphous oligo(L-lactic acid) with a short chain length was grafted through the backbone of CS. Notably, this will provide a convenient method to combine the bioactive functions of CS with the good mechanical properties of biodegradable polymers, which could be rationally designed in advance.

Solubility of CS-*g*-PLLA. In comparison with the original CS, the CS-*g*-PLLA copolymers exhibited good solubility in some common organic solvents including nonpolar and polar solvents (Table 2). This indicates that the PLLA grafts with a long chain length not only improved the hydrophobicity−hydrophilicity balance of the CS-*g*-PLLA amphiphiles, but also probably reduced the inter- and/or intramolecular hydrogen bonds of the CS backbone. This improved solubility will facilitate the CS-*g*-PLLA biohybrid to be easily fabricated into various micro- and/or nanoparticles, which have been widely used for biomedical applications.

Self-Assembly Properties. To investigate the self-assembly properties of CS-*g*-PLLA amphiphiles, we first examined their

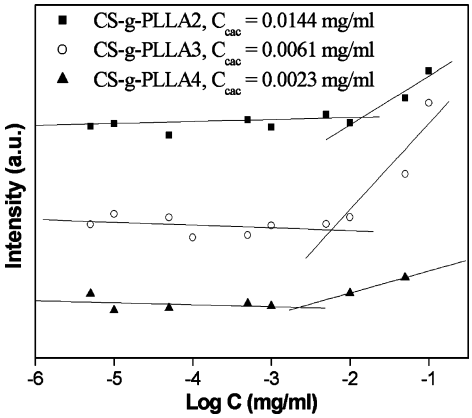

Figure 7. Relationship of the absorbance intensity of DPH as a function of the graft copolymer concentration at room temperature.

Table 3. Nanoparticles with Adjustable Sizes Fabricated from CS-*g*-PLLA Amphiphiles

sample	av diam (c = 2.5 mg/mL)[a]	av diam (c = 5.0 mg/mL)[a]	av diam (c = 10.0 mg/mL)[a]
CS-*g*-PLLA1	14.8 ± 3.01	25.2 ± 1.82	42.0 ± 5.38
CS-*g*-PLLA2	33.1 ± 4.17	56.5 ± 3.40	75.6 ± 6.02
CS-*g*-PLLA3	44.5 ± 5.13	66.6 ± 6.21	85.6 ± 3.72
CS-*g*-PLLA4	65.1 ± 2.42	80.3 ± 1.01	102.9 ± 1.98

[a] These nanopaticles were generated by direct injection of CS-*g*-PLLA copolymer solutions at 2.5, 5.0, and 10.0 mg/mL into distilled water, respectively.

cac employing the dye solubilization method. The relationship of the absorbance intensity of the DPH probe molecule as a function of the graft copolymer concentration at room temperature is shown in Figure 7. It can be seen that the absorbance intensity values of DPH remained nearly constant below a certain concentration. Above that concentration, the intensity increased substantially, reflecting the incorporation of DPH into the hydrophobic region of the aggregates. The cac value of the CS-*g*-PLLA amphiphiles decreased with increasing number of PLLA grafts per CS, which was similar to that reported in amphiphilic block copolymers.[24]

The DLS analysis of these aggregates is shown in Table 3 and Figure 8. At a graft copolymer concentration of 5 mg/mL in solution, the average diameter of the aggregates was in the range of 25.2−80.3 nm for all CS-*g*-PLLA samples. This indicates that the average diameter of the aggregates apparently increased with increasing number of PLLA grafts per CS, which was attributed to the increased surface tension resulting from the increased hydrophobicity−hydrophilicity balance.[25,26] Notably, this is very different from the observations for biodegradable and amphiphilic PLLA-*b*-PEO and/or poly(ϵ-caprolactone)-*b*-PEO systems, where different copolymer compositions would mainly induce the morphological evolution of self-assembled aggregates (e.g., the morphology typically changed from spherical micelles to cylinders to vesicles).[5] Moreover, the average diameter of the aggregates increased with increasing graft copolymer concentration in solution (e.g., CS-*g*-PLLA2 and CS-*g*-PLLA4 at different graft copolymer concentrations, Table 3). This suggested that the concentration of the CS-*g*-PLLA graft copolymer in solution was also an important factor in controlling the size of self-assembled nanoparticles.[27] Note that a certain amount of bigger aggregates (about 650 nm) were present in the nanoparticle solution (see Supporting Information Figure S4), which was usually observed in the fabrication of nanoparticles.[28,29] The morphology of these aggregates was further

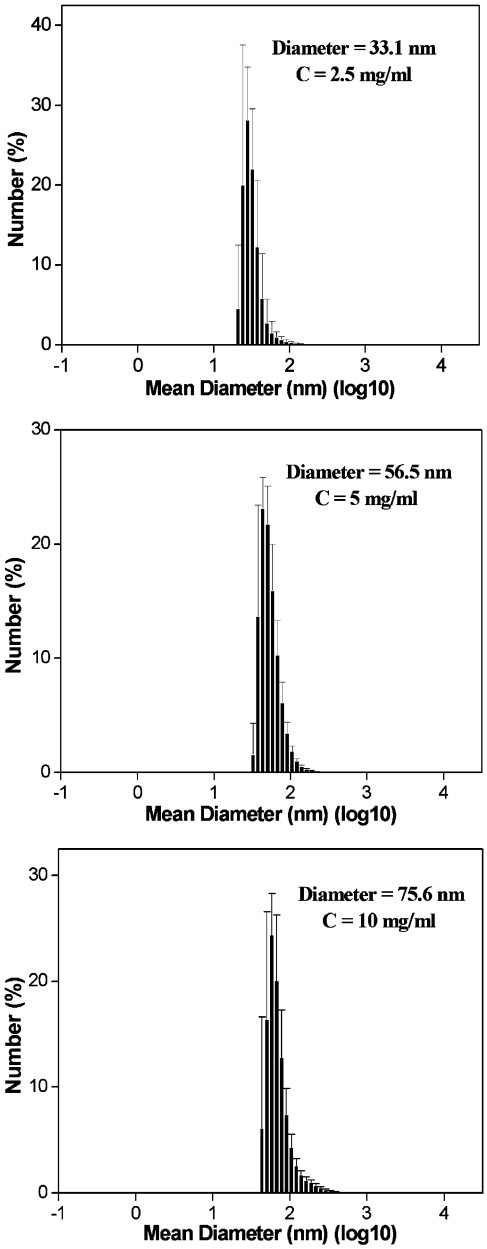

Figure 8. Nanoparticle size distribution of CS-*g*-PLLA2 amphiphiles at different copolymer concentrations in solution.

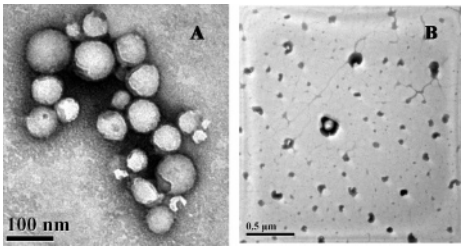

Figure 9. TEM photographs of CS-*g*-PLLA2 (A) and CS-*g*-PLLA4 (B) amphiphiles.

observed by TEM using negative staining, as shown in Figure 9. CS-*g*-PLLA2 gave the normally spherical micelles with an average size of ~65 nm, which was nearly consistent with the DLS analysis. Note that CS-*g*-PLLA4 showed mainly spherical micelles and some irregular nanoaggregates, which might be attributed to the large differences in the number of PLLA grafts per CS. In all, these results indicate the biodegradable nanoparticles with adjustable sizes (25−103 nm) can be easily

generated from CS-*g*-PLLA hybrid amphiphiles, and they completely meet the size prerequisite for targeted drug delivery.[17]

Conclusions

Biodegradable CS-*g*-PLLA amphiphiles with a long chain length of PLLA were successfully prepared via a graft-to strategy. The average number of PLLA grafts per CS molecule could be easily adjusted by the feed ratio of PLLA to CS. Moreover, both the crystallization rate and degree of crystallization of these CS-*g*-PLLA copolymers could be adjusted by the chain length of PLLA and the number of PLLA grafts per CS, respectively, which are important parameters for adjusting the biodegradation rate and mechanical properties of biodegradable polymers. Furthermore, the average size of the micelles could be adjusted through the graft copolymer composition and the graft copolymer concentration. Significantly, this will provide a convenient method not only to combine the bioactive functions of CS with the good mechanical properties of biodegradable polymers, but also to generate nanoparticles with adjustable sizes for targeted drug release.

Acknowledgment. We are grateful for the financial support of the key research project of the Shanghai Science and Technology Committe (Grant 05DJ14005) and the National Natural Science Foundation of China (Grant 20404007) and for the assistance of the Instrumental Analysis Center of Shanghai Jiao Tong University.

Supporting Information Available. ^{1}H NMR spectrum for PLLA−NCO and ^{13}C NMR, GPC, and DLS results for CS-*g*-PLLA3. This material is available free of charge via the Internet at http://pubs.acs.org.

References and Notes

(1) He, Y.Y.; Li, Z. B.; Simone, P.; Lodge, T. P. *J. Am. Chem. Soc.* **2006**, *128*, 2745−50.
(2) Gaucher, G.; Dufresne, M. H.; Sant, V. P.; Kang, N.; Maysinger, D.; Leroux, J. C. *J. Controlled Release* **2005**, *109*, 169−88.
(3) Discher, D. E.; Eisenberg, A. *Science* **2002**, *297*, 967−73.
(4) Akiyoshi, K.; Maruichi, N.; Kohara, M.; Kitamura, S. *Biomacromolecules* **2002**, *3*, 280−283.
(5) Ahmed, F.; Discher, D. E. *J. Controlled Release* **2004**, *96*, 37−53.
(6) Wang, L. Y.; Ma, G. H.; Su, Z. G. *J. Controlled Release* **2005**, *106*, 62−75.
(7) Kumar, M. N.; Muzzarelli, R. A.; Muzzarelli, C.; Sashiwa, H.; Domb, A. J. *Chem. Rev.* **2004**, *104*, 6017−84.
(8) Kweon, D. K.; Song, S. B.; Park, Y. Y. *Biomaterials* **2003**, *24*, 1595.
(9) Wu, Y.; Zheng, Y.; Yang, W.; Wang, C.; Hu, J.; Fu, S. *Carbohydr. Polym.* **2005**, *59*, 165−71.
(10) Liu, L.; Wang, Y.; Shen, X.; Fang, Y. *Biopolymers* **2005**, *78*, 163−70.
(11) Fujioka, M.; Okada, H.; Kusaka, Y.; Nishiyama, S.; Noguchi, H.; Ishii, S.; Yoshida, Y. *Macromol. Rapid Commun.* **2004**, *25*, 1776−80.
(12) Dechy-Cabaret, O.; Martin-Vaca, B.; Bourissou, D. *Chem. Rev.* **2004**, *104*, 6147.
(13) Cai, Q.; Zhao, Y. L.; Bei, J. Z.; Wang, S. G. *Biomacromolecules* **2003**, *4*, 828.
(14) Qu, X.; Wirse'n, A.; Albertsson. A. C. *Polymer* **2000**, *41*, 4841−47.
(15) Qu, X.; Wirse'n, A.; Albertsson. A. C. *J. Appl. Polym. Sci.* **1999**, *74*, 3186−72.
(16) Yao, F.; Liu, C.; Chen, W.; Bai, Y.; Tang, Z.; Yao, K. *Macromol. Biosci.* **2003**, *3*, 653−56.
(17) Haag R. *Angew. Chem., Int. Ed.* **2004**, *43*, 278−82.
(18) Wang, L.; Dong, C. M. *J. Polym. Sci., Part A: Polym. Chem.* **2006**, *44*, 2226−36.
(19) Park, S. Y.; Han, B. R.; Na, K. M.; Han, D. K.; Kim, S. C. *Macromolecules* **2003**, *36*, 4115−24.
(20) Jenkins, D. W.; Hudson, S. M. *Chem. Rev.* **2001,** *101*, 3245−73.
(21) Cai, C.; Wang, L.; Dong, C. M. *J. Polym. Sci., Part A: Polym. Chem.* **2006**, *44*, 2034−44.
(22) Wang, J. L.; Dong, C. M. *Polymer* **2006**, *47*, 3218−28.
(23) Tsuji, H.; Ogiwara, M.; Saha, S. K.; Sakaki, T. *Biomacromolecules* **2006**, *7*, 380−87.
(24) Vangeyte, P.; Leyh, B.; Heinrich, M.; Grandjean, J.; Bourgaux, C.; Jerome, R. *Langmuir* **2004**, *20*, 8442−51.
(25) Gao, H.; Wang, Y. N.; Fan, Y. G.; Ma, J. B. *J. Controlled Release* **2005**, *107*, 158−73.
(26) Dong, Y.; Feng, S. S. *J. Biomed. Mater. Res.* **2006**, *78A*, 12−19.
(27) Cho, E. C.; Cho, K.; Ahn, J. K.; Kim, J.; Chang, I. S. *Biomacromolecules* **2006**, *7*, 1679−85.
(28) Allen C.; Yu, Y.; Maysinger, D.; Eisenberg, A. *Bioconjugate Chem.* **1998**, *9*, 564−72.
(29) Hu, Y.; Jiang, X.; Ding, Y.; Zhang L.; Yang, C.; Zhang, J.; Chen, J.; Yang, Y. *Biomaterials* **2003**, *24*, 2395−2404.

BM060568L